

**TIME-RESOLVED PHOTOACOUSTIC SPECTROSCOPY OF WATER  
VAPOR AND SOOT AEROSOL IN ATMOSPHERIC AIR<sup>1</sup>**

B.A. Tikhomirov<sup>2</sup>

<sup>1</sup>Paper presented at the Fifteenth Symposium on Thermophysical Properties, June 22-27, 2003, Boulder, Colorado, U.S.A.

<sup>2</sup>Siberian Branch of the Russian Academy of Sciences, Institute of Atmospheric Optics  
Akademicheskii Ave. 1, 634055 Tomsk, Russia

E-mail: [bat@iao.ru](mailto:bat@iao.ru)

## ABSTRACT

In the paper method of photoacoustic spectroscopy with time-resolution of signals is applied to study the short-wave radiation absorption by the soot aerosol in the ground atmosphere and the collision relaxation of excited molecules by the example of water vapor. As the result of synchronous measurements of aerosol absorption coefficients with a pulsed photoacoustic spectrometer and mass concentration of soot with an aethalometer, we have obtained values of efficiency of radiation absorption by soot particles in the atmospheric air in the short-wave spectral range for three wavelengths:  $\sigma(532 \text{ nm}) = (4.61 \pm 2.35) \text{ m}^2 \cdot \text{g}^{-1}$ ,  $\sigma(694 \text{ nm}) = (3.75 \pm 1.68) \text{ m}^2 \cdot \text{g}^{-1}$ , and  $\sigma(1064 \text{ nm}) = (2.41 \pm 1.21) \text{ m}^2 \cdot \text{g}^{-1}$ . The experimental results are approximated by the spectral dependence  $\sigma(\lambda) = 2.61 \cdot \lambda^{-0.92}$ , where  $\lambda$  is wavelength. Procedure of the pulse photoacoustic spectrometers calibration on the known molecular absorption in the study of aerosol absorption is discussed. The collision relaxation time of  $\text{H}_2\text{O}(\nu_1 + 3\nu_3)$  molecules was determined in two ways from the following pressure dependencies: the oscillation phase of microphone membrane and duration of the photoacoustic signal compression pulse.

**KEY WORDS:** pulse photoacoustic spectroscopy, relaxation of vibrational excited molecules in gases, absorption by ambient soot aerosol

## INTRODUCTION

The photoacoustic (PA) method of laser spectroscopy is widely used to measure a weak absorption in molecular gases and fluids and to detect pollutants, and to study kinetic processes in that substances [1-3].

The accurate experimental data on spectral dependence of weak soot aerosol absorption in atmospheric air are very needed for development of radiance models of atmosphere. The available present-day data are contradictory. For example, the experimental dependence of the efficiency of soot aerosol absorption  $\sigma(\lambda) \sim \lambda^{-1}$  is reported by Bergstrom et al. [4]. Experiments in that case were carried out through sinking the aerosol samples from the atmospheric air on the filters and consequent recording of their absorption spectra within the wavelengths range  $\lambda = (0.4 - 1) \mu\text{m}$ . Experiments made by the method of resonance PA laser spectroscopy [5], gave some what other spectral dependence  $\sigma(\lambda) \sim \lambda^{-2.7}$  in the range  $\lambda = (0.4 - 0.8) \mu\text{m}$ .

Usually the data on constants of collisional relaxation of molecules in gases are received for the fundamental vibrational states of exited molecules by the use of PA, fluorescence, double-resonance techniques etc. Because of the weak molecular absorption in the Visible such data are practically absent for high-energy vibrational states in the references. This information is needed to study the kinetic processes in the upper atmosphere.

High sensitivity and sufficient time resolution of PA spectrometers with pulse lasers and comparatively big cells allows us to obtain the following advantages when the weak absorption in gases is studied:

- to eliminate the influence of unwanted PA signals and to detect absorption in gas at zero background in any spectral range;
- to increase the sensitivity of pulse OA spectrometers more than one order, working with acoustic mirrors used to focus the pressure pulses. In this case the value of minimal detectable absorption coefficient  $k^{\text{min}} \sim 10^{-11} \text{ cm}^{-1}$  can be achieved when the laser pulse energy  $E = 1 \text{ J}$ ;
- to study the fast relaxation of exited molecules from upper vibrational states.

In the present paper these advantages are used in study of spectral dependence of soot aerosol absorption in atmospheric air and in measurements of relaxation time of water vapor molecules.

### 1. PA SIGNAL WAVEFORM SIMULATION

The waveform of PA pressure pulses in liquids and gases are usually simulated by numerical integration of the wave equation solution [6-8]. Linear approximation is considered [6], as electrostriction [7] and nonlinear thermal expansion [8] are taken into account. Generally PA signal is described by the wave equation for pressure  $p(r, t)$ :

$$\frac{\partial^2 p(r, t)}{\partial t^2} - V_s^2 \nabla^2 p(r, t) = (\gamma - 1) \frac{\partial I(r, t)}{\partial t}, \quad (1)$$

where  $V_s$  is the sound speed,  $\gamma$  is the ratio of heat capacities, and  $I(r, t)$  is the speed of heat release in volume unit. When Gaussian laser beam is under discussion and heat release process is described by the function  $f(t)$ , so:

$$I(r, t) = W \exp\left(-\frac{r^2}{2 r_0^2}\right) f(t) \quad (2)$$

the general solution of the wave equation is given by the formula:

$$p(r, t) = (\gamma - 1) \int_{-\infty}^t dt' \int_0^{\infty} r' dr' \int_0^{\infty} k dk I(r', t') \cos[k V_s(t - t')] J_0(kr) J_0(kr'), \quad (3)$$

where  $J_0$  is the Bessel function,  $r_0$  is the laser beam radius,  $W$  is the energy density emerged in the center of laser beam. When the far-field approximation is considered, i.e.  $r_0 \ll r$  where  $r$  is the distance from the laser beam to the point of observation, the last equation is transformed to:

$$p(r, t) = (\gamma - 1) W \int_{-\infty}^t f(t') dt' \int_0^{\infty} k^{1/2} dk \exp\left(-\frac{k^2 r_0^2}{2}\right) \cos\left\{k[r - V_s(t - t')] - \frac{\pi}{4}\right\} \quad (4)$$

This equation describes the PA pressure pulse waveform as a function of spatial and time parameters of the laser beam, thermodynamic, and kinetic properties of medium. The shapes of  $p(r, t)$  calculated using the expression (4) for exponential and Gaussian heat release processes are shown in Figures 1(a) and 1(b). The pressure signal consists of compression and rarefaction pulses. The shapes of signals are practically equal when duration of heat release  $\tau = 1 \mu\text{s}$  and are differed in a little when  $\tau = 10 \mu\text{s}$ .

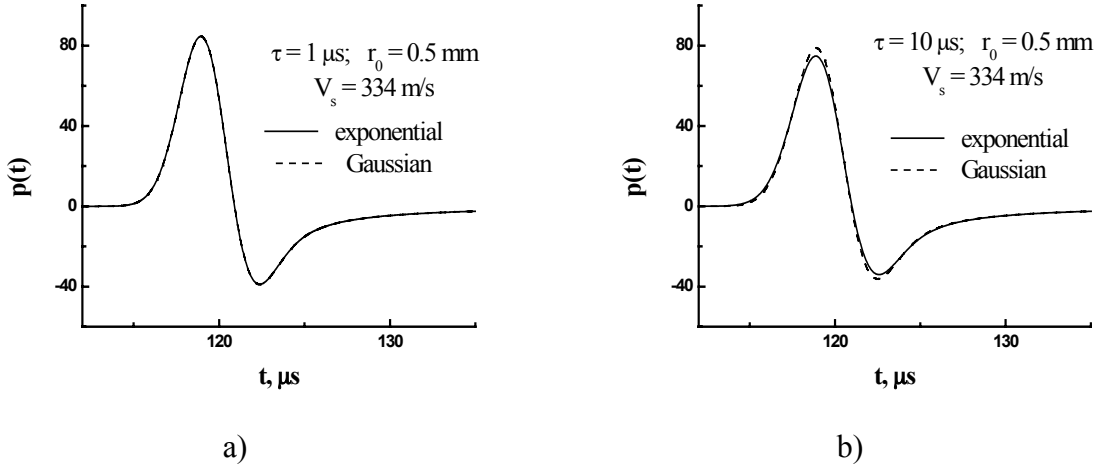


Fig.1. Shape of PA pressure signal for exponential  $f(t) = 1 - \exp(-t/\tau)$  and Gaussian  $f(t) = \exp(-t^2/\tau^2)$  heat release processes. The laser pulse duration  $\tau_p \ll \tau$ .

## 2. EXPERIMENT

### 2.1. PA spectrometer

The general-purpose PA spectrometer's schematic is presented in Figure 2. The set-up consists of the pulse solid-state laser (ruby or Nd:YAG) and PA detector with the blocks of electrical signal amplification and recording. The digital S9-16

oscilloscope with the bandwidth of 20 MHz allows us to record the shape of PA signal. Fabry-Perot interferometer analyzer of spectrum is used to measure laser radiation spectral characteristics. Time evolution of laser's pulses is recorded with the FK-19 photodetector and high-speed S7-19 oscilloscope with a resolution of  $\sim 1$  ns. The laser pulse energy is measured with IKT-1H calorimeter located behind the PA sell.

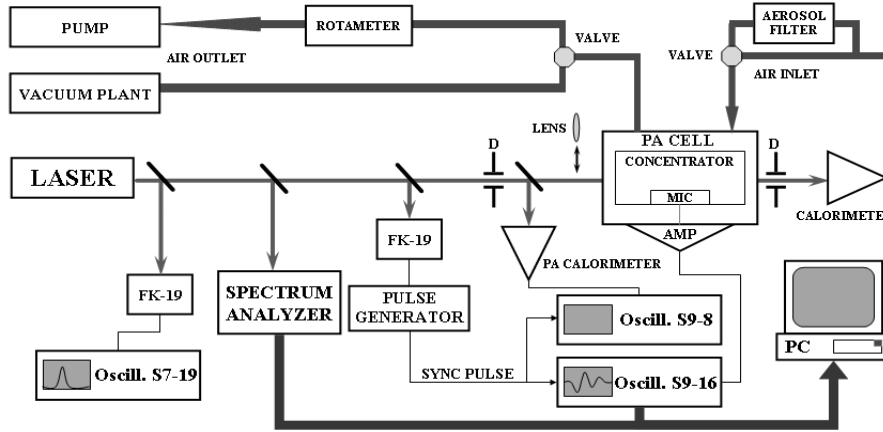


Fig.2. Experimental set-up of pulse PA spectrometer.

A vacuum plant served to pump out the gas from the cell of the PA detector, to prepare water vapor-buffer gas mixture and flow it into the cell. Sampling the atmospheric air into the cell was done by means of a bleeding block.

All necessary information on parameters of the recorded pulses and measurement conditions entered a computer.

**Lasers.** The frequency tunable ruby laser is described in detail in Ref. [9]. When calibrating the spectrometer or measuring the relaxation time of  $\text{H}_2\text{O}$  ( $\nu_1 + 3\nu_3$ ) molecules, the laser was tuned in resonance with water vapor absorption line of 694.380 nm. When measuring the aerosol absorption coefficient in air, it was tuned at the wavelength of 694.300 nm close to minimum of molecular absorption of radiation by the atmospheric air in that spectral range. The Nd:YAG-laser construction was similar to that of driving oscillator of the laser system constructed by Tyryshkin et al. [10]. Transformation of the 1064 nm radiation into the second harmonics (532 nm) was done by the KTP crystal with the efficiency up to 60%.

Laser pulse characteristics are presented in Table 1.

Table 1. Characteristics of pulse lasers.

Laser	$\lambda$ , nm	E, mJ	$\tau$ , ns
ruby	694.1 – 694.5	30	50
Nd:YAG	532	30	5
	1064	55	5

**PA detectors.** The detector used to study the relaxation processes in molecular gases includes a cylindrical cell of 200 mm in diameter and 300 mm length. Its end-windows have transparent windows for radiation input and output. A quarter-inch capacitor microphone MK-301 (“Robotron”) with resonance frequency of membrane oscillations

at low pressure of gas in the cell  $\omega = 2 \cdot \pi \cdot f \approx 350$  kHz was placed in the center of the cell.

The cell construction used to measure the aerosol absorption coefficients, schematically shown in Figure 3, additionally includes an acoustic concentrator consisting of two parabolic mirrors. The concentrator is analogous to that suggested by Carrer et al. [11]. The laser radiation beam axis coincides with the focal axis of the cylindrical paraboloid characterized by the focus length of 10 mm and the reflecting surface area of

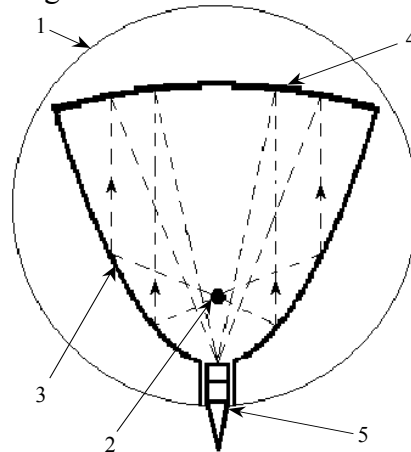


Fig. 3. Scheme of PA cell with concentrator of the acoustic pulse energy: cell body (1), laser beam (2), cylindrical paraboloid (3), spherical paraboloid (4), microphone (5).

$150 \times 210 \text{ mm}^2$ . A half-inch capacitor microphone MK-201 (“Robotron”) with bandwidth of 20 kHz, placed in the spherical paraboloid’s focus, records a pressure pulse amplified after its reflection from the mirrors. Focus length of spherical paraboloid equals to 100 mm. Sizes of the cell and acoustic mirrors were chosen in order to share in time the useful and unwanted signals. The use of the concentrator allowed us to achieve more than an order of magnitude enhancement of sensitivity of the PA detector.

**Selection of laser radiation parameters.** The pulse laser spectrometer sensitivity depends on the location of laser beam relative to the microphone [6-8]. In the PA cell with concentrator, used in this work, it depends on the laser beam location relative to the focal axis of the cylindrical paraboloid. We have noted that some small changes in alignment of PA cell relative to the radiation beam result in large changes in the spectrometer’s sensitivity. To make it stable, for example, when changing laser sources, a portion of radiation was directed with the help of thin beam splitter placed in front of the cell (see Fig. 2), to the PA calorimeter, which served to measure laser pulse energy in relative units. The diaphragm of 3.5 mm in diameter was put in front of the cell at the distance of 0.5 m of the input window. Precisely the same diaphragm was located between the cell and the IKT-1H calorimeter at the range of 0.5 m of the output window. Such a scheme allowed us to align the laser relative the fixed cell by the ratio of the calorimeters’ readings, as well as to get equal sensitivities of spectrometer with different lasers.

Moreover, the shape of the pressure pulse, and, consequently, sensitivity of the PA spectrometer depend on time-space parameters of a laser beam, as well as thermodynamic characteristics of gas in the cell [6-8].

Relaxation of H<sub>2</sub>O excited molecules from the vibrational excited state ( $v_1 + 3v_3$ ) in air at  $P = 760$  torr is characterized by the vibrational-translational time  $\tau_{VT} \approx 10^{-8}$  s. The time of thermalization of an aerosol soot particle, heated by a radiation pulse, in air can be estimated from the relation [12]:  $\tau_s = \rho_s \cdot r_s^2 \cdot C_s / 3k_a$ , where  $k_a$  is the heat conductivity of air;  $\rho_s$ ,  $C_s$ , and  $r_s$  are the density, heat capacity and radius of a spherical soot particle, respectively. Maximum of the size distribution for the soot particles under study falls on the value range  $r_s \sim 120$  nm [13]. In this case we have for the soot particles thermalization time  $\tau_s = 2.2 \cdot 10^{-7}$  s. We used following reference data in our estimates:  $k_a = 0.0257 \text{ W} \cdot \text{m}^{-1} \cdot \text{K}^{-1}$ ,  $\rho_s = 1.88 \cdot 10^3 \text{ kg} \cdot \text{m}^{-3}$ , and  $C_s = 641 \text{ J} \cdot \text{kg}^{-1} \cdot \text{K}^{-1}$ .

Thus, in our experiments, the law of heat emission process in air after absorption of ruby laser and Nd:YAG-laser radiation by soot particles is exponential with duration  $\tau_s = 2.2 \cdot 10^{-7}$  s. When calibrating the spectrometer by molecular absorption of the ruby laser radiation by water vapor in air at the atmospheric pressure, the heat emission process law is determined by the Gaussian shape of laser pulse and its duration is close to that of the laser pulse  $\tau \sim 5 \cdot 10^{-8}$  s.

Figure 4(a) plots the dependence of the pressure signal amplitude  $p_{\max}$  on the laser beam radius  $r_0$  for three heat emission laws (Gaussian, exponential, and rectangular) at  $\tau = 5 \cdot 10^{-8}$  s and  $\tau = 10^{-6}$  s. Similar dependencies for the compression pulse duration of the PA signal at the half-height  $\tau_{0.5}$  are given in Figure 4(b).

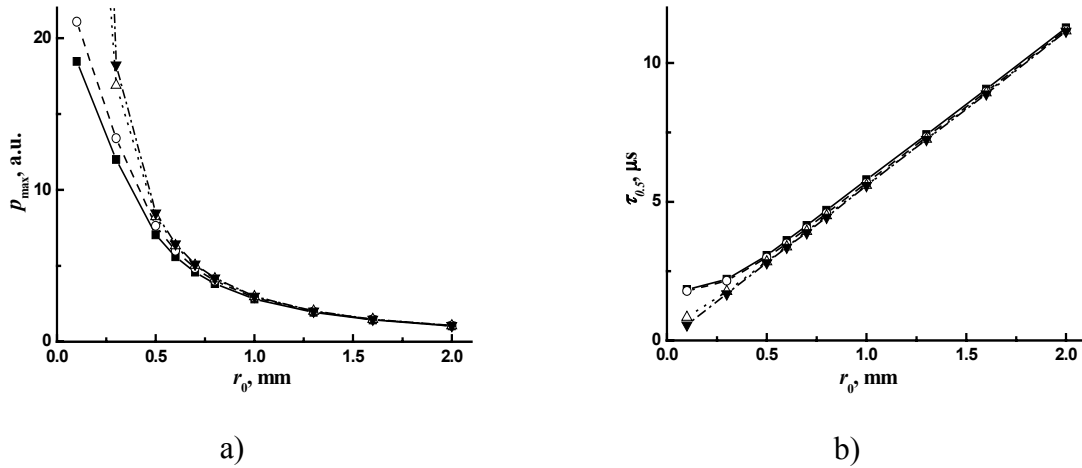


Fig.4. a) - Dependencies of the compression pulse amplitude of PA pressure signal  $p_{\max}$  on the laser beam radius  $r_0$  for three laws of heat emission at  $\tau = 10^{-6}$  s: exponential (squares), Gaussian (circles), rectangular (light triangles), the same at  $\tau = 5 \cdot 10^{-8}$  s (dark triangles).  
b) - The same for compression pulse duration of PA pressure signal  $\tau_{0.5}$

They were obtained by numerical calculations with the use of expression (4). It is seen that as  $r_0$  increases, the amplitude and duration of the compression pulse of the pressure signal, beginning from  $r_0 \sim 1$  mm, become independent of heat emission pulse's shape and duration. That is, at  $r_0 \approx 1.75$  mm, used in these measurements, there is a good reason to believe that the PA spectrometer's sensitivity is the same both in measuring the molecular absorption of pulse laser radiation by water vapor and in measuring the absorption by aerosol particles.

In measurements of water vapor relaxation time the lens with focal length of 0.3 m was placed in front of the PA cell so the position of lens relative to microphone allows us to choose the diameter of laser beam in region near microphone.

**Calibration of the PA spectrometer.** Calibration of the spectrometer to measure aerosol absorption in atmospheric air is described in detail in Ref. [9]. To do this, the ruby laser was tuned in the resonance with the H<sub>2</sub>O absorption line of 694.380 nm, to which the achievement of the PA signal amplitude maximum  $U^{\max}$  corresponds. Then the gas was pumped out of the cell and the cell was washed by nitrogen until the PA signal amplitude  $U^{\max}$  decreases to zero. Pumping out the gas of the cell continued up to the pressure  $P_{\text{tot}} \leq 0.02$  torr. Then the cell was successively filled with certain amount of water vapor from a balloon with distilled water and by room air. The water vapor content in air was measured with the use of Assmann hygrometer. The resulting pressure in the cell was equal to the atmospheric one. Like in Ref. [9], in the present experiment the spectral distribution of  $(U \cdot E^{-1})$  was recorded and the value of  $(U^{\max} \cdot E^{-1})$ , corresponding to absorption at the 694.380 nm line center, was determined. By results of measurements of the resonance absorption at several values of air humidity, we have built the function  $(U^{\max} \cdot E^{-1})$  of the efficient absorption coefficient, which is proportional to the partial pressure of water vapor in the mixture. To calculate the values of efficient absorption coefficient the data on the intensity  $S$  and the coefficient of the line broadening by air  $\gamma$ , obtained Ref. [14] with the use of laser spectrophotometer based on a multi-pass cell with the optical path length up to 4 km:  $S = (4.54 \pm 0.27) \cdot 10^{-24} \text{ cm} \cdot \text{mol}^{-1}$  and  $\gamma = (3.52 \pm 0.35) \text{ MHz} \cdot \text{torr}^{-1}$  are chosen. The PA spectrometer's sensitivity  $\alpha = (3.7 \pm 0.9) \cdot 10^7 \text{ V} \cdot \text{cm} \cdot \text{J}^{-1}$  was found from the slope of the function. Such sensitivity allows the minimal absorption coefficient  $k^{\min} = 6.8 \cdot 10^{-11} \text{ cm}^{-1}$  to be detected at the laser pulse energy  $E = 1 \text{ J}$  and at the noise level of our PA detector  $U_n = 2.5 \text{ mV}$ .

## 2.2. Aethalometer

The real-time measurements of the soot mass concentration  $M_s$  ( $\mu\text{g}/\text{m}^3$ ) in the atmospheric air were carried out with the use of aethalometer [15]. Absolute calibration of the aethalometer was based on comparison of data of optical and gravimetric measurements. In the calibration soot particles of 50–200 nm in size formed at pyrolysis of butanol vapors in the nitrogen atmosphere at a temperature of 1150°C were used. The determined value of the calibration constant for the aethalometer  $K = (16.1 \pm 3.2) \text{ cm}^2 \cdot \mu\text{g}^{-1}$  shows that the aethalometer can record minimal surface concentration of soot on the filter of about  $1.5 \text{ ng} \cdot \text{cm}^{-2}$ . This means that when flowing through a cell approximately 35 liters of air, the minimally recorded concentration of soot in air (ultimate sensitivity of the instrument) is about  $0.02 \mu\text{g} \cdot \text{m}^{-3}$ . To decrease the threshold of sensitivity, it is necessary to increase the volume of the flowing air. In its turn, the upper limit of measurements of soot large concentrations is limited by the saturation effect, when the reached values of the surface soot concentration on the filter are about  $8 \mu\text{g} \cdot \text{m}^{-2}$ . The upper limit can be improved due to decrease of air volume. The measurement error within the range of soot particle concentrations in air  $0.1$  to  $4.5 \mu\text{g} \cdot \text{m}^{-3}$  does not exceed 20% [15].

### 3. APPLICATION TO STUDY OF AEROSOL ABSORPTION IN ATMOSPHERIC AIR

#### 3.1. Synchronous measurements of the aerosol absorption coefficient and mass concentration of soot aerosol in air.

Synchronous measurements were done with the use of the above-described instrumentation every 15 minutes. The PA spectrometer and aethalometer were located in a working room of the Institute of Atmospheric Optics SB RAS (eastern outskirts of Tomsk city). Sampling the atmospheric air was performed by pumping it to cells through pipes from the intake located 3 m above the ground. The time of air flowing through the aethalometer's filter was 7 min. The flowing rate of 3 l/min was set prior air sampling. Air consumption during its flowing through the PA cell was 10 l/min. Air flowing through the PA cell started 3 min earlier than through aethalometer and longed for 10 min. These parameters (duration and flow rate) of air sampling were pre-chosen experimentally and provided a good correlation between instruments' readings in synchronous experiments.

In the process of air flowing through the aethalometer the apparatus recorded value for the flowing time concentration of soot particles in air. The resulting value corresponding to 7 minute-averaged soot concentration was recorded by a computer. Measuring aerosol absorption coefficients with PA spectrometer was made after accumulating PA signals for 10 laser pulses. This allowed us not only to exclude random peaks, but also to increase the signal-to-noise ratio by factor 3.3. Every series of measurements was ended by flowing air through aerosol filters. In this case, the instrument readings were taken in the absence of soot particles in air.

#### 3.2. Spectral dependence of soot aerosol absorption efficiency.

Results of the synchronous measurements of the aerosol absorption coefficient for 694.300 nm wavelength and mass concentration of soot aerosol in air are given in Figure 5(a). It is seen that the absorption coefficient is changed synchronously with time variation of soot particle concentrations in atmospheric air. Observable in Figure 5(a) residual absorption by the atmospheric air flown through the aerosol filter is due to radiation absorption by water vapor. In this case, the measured value of absorption coefficient  $k^{\text{meas}} = 1.33 \cdot 10^{-8} \text{ cm}^{-1}$  is in good agreement with  $k^{\text{calc}} = 1.11 \cdot 10^{-8} \text{ cm}^{-1}$  calculated for partial pressure of water vapor  $P_{\text{H}_2\text{O}} = 2.0$  torr in the air under study.

Figure 5(b) demonstrates correlation between the aerosol absorption coefficient for this wavelength and mass concentration of the soot aerosol in air. Analogous pictures were obtained for wavelengths of 532 nm and 1064 nm.

Taking into account the PA spectrometer and aethalometer calibration errors (23% and 20%, respectively), we have found the following values of efficiencies of the radiation absorption by the soot aerosol in the atmospheric air:  $\sigma(532 \text{ nm}) = (4.61 \pm 2.35) \text{ m}^2 \cdot \text{g}^{-1}$ ,  $\sigma(694 \text{ nm}) = (3.75 \pm 1.68) \text{ m}^2 \cdot \text{g}^{-1}$ , and  $\sigma(1064 \text{ nm}) = (2.41 \pm 1.21) \text{ m}^2 \cdot \text{g}^{-1}$ .

Figure 6 presents the data on determination of efficiencies of short-wave radiation absorption by soot particles in air after synchronous measurements of aerosol absorption coefficients and mass concentrations of soot particles in air. Our data are presented in Figure 6 by squares. These data are approximated by the spectral dependence close to

the theoretical one:  $\sigma(\lambda) = \lambda^{-1}$ . The same dependence is resulted from the filter measurements of spectral behavior of the short-wave radiation absorption by artificial and atmospheric soot particles [4].

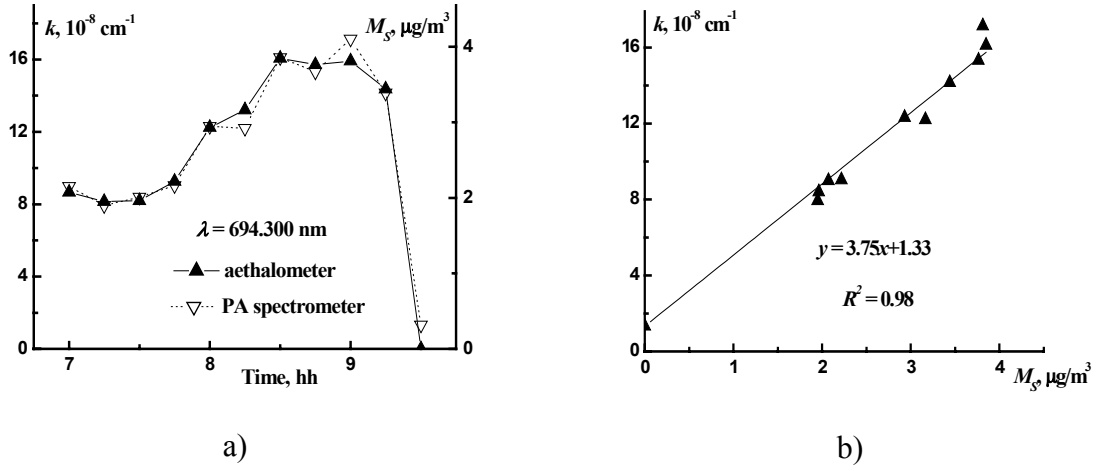


Fig.5. a) - Dependence of aerosol absorption coefficient  $k$  for 694.300 nm wavelength (light triangles) and mass concentration  $M_s$  of soot particles in the atmospheric air (dark triangles) on the time of sampling. The later in time point corresponds to the instrument's readings after air intaking through aerosol filter. b) - Correlation between  $M_s$  and  $k$  when  $\lambda = 694 \text{ nm}$ . Soot aerosol absorption efficiency is found to be  $\sigma(694 \text{ nm}) = (3.75 \pm 0.07) \text{ m}^2 \cdot \text{g}^{-1}$  from the slop of fitted linear regression.

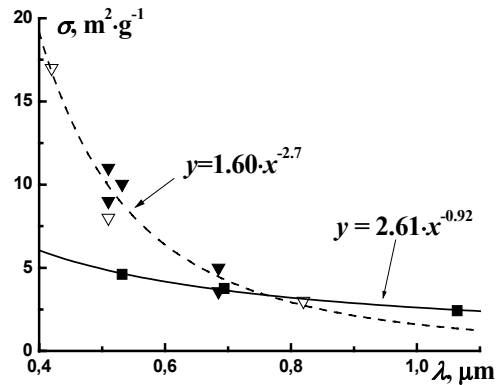


Fig.6. Dependence of the efficiency  $\sigma$  of the short-wave radiation absorption by soot aerosol in air on  $\lambda$ . Data of measurements [5] (triangles) are approximated by  $y = 1.60 \cdot x^{-2.71}$  with  $R^2 = 0.95$ . Results of present measurements (squares) are approximated by  $y = 2.61 \cdot x^{-0.92}$  with  $R^2 = 0.98$ .

Data taken from the paper of Moosmuller et al. [5] are denoted by triangles. Dark triangles present the values of efficiency for ambient soot particles, and light ones present the same for artificial soot particles. These data are approximated by the essentially other dependence:  $\sigma(\lambda) \sim \lambda^{-2.7}$ . We believe that radiation scattering by

aerosol particles in the resonance PA sells with further absorption of the scattered radiation by the cells walls are the main reasons to find a such spectral dependence.

### 3. APPLICATION TO STUDY OF FAST RELAXATION IN MOLECULAR GASES

#### 3.1. Determination of relaxation time for H<sub>2</sub>O (ν<sub>1</sub> + 3ν<sub>3</sub>) over the phase of pulse PA signal oscillations.

Under the low gas pressure in the PA cell ( $P \leq 100$  torr), very sharp resonance in the microphone frequency response is appeared. In this case under the action of the short radiation pulse with the duration  $\tau \ll \tau_{VT}$  the electrical signal of PA detector has the shape presented in Figure 7(a).

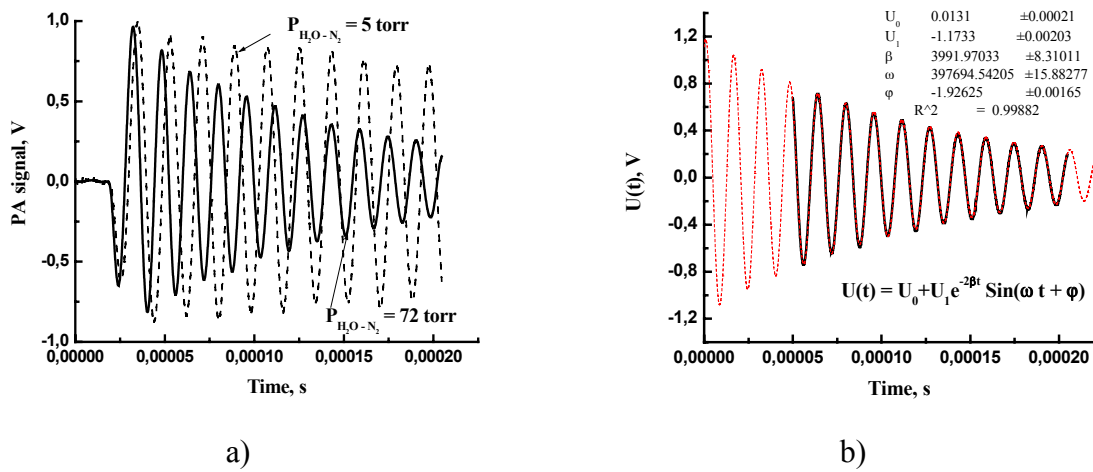


Fig.7. a) - PA detector signals for different pressures of H<sub>2</sub>O-N<sub>2</sub>-mixture in the cell.  
b) - Determination of fit parameters for free oscillations of microphone membrane.

The frequency of damped oscillations observed in the signal is equal to the basic natural frequency of membrane oscillations. Increasing of gas pressure in the cell produces the increasing of oscillations damping factor and frequency and decreasing of phase delay. One of the reason of phase delay dependency on the pressure is that relaxation time of absorbing molecules depends on the pressure. This effect was suggested to use in measurements of relaxation time of vibration excited molecules in Ref. [16]. Such oscillations parameters as an amplitude  $U_0$ , frequency  $\omega$ , phase delay  $\phi$ , and damping factor  $\beta$  are determined with high accuracy as results of computer processing of the electrical signal time-base part corresponded to the membrane undisturbed oscillations (see Fig.7(b)). PA signal phase delay is calculated relatively to point of laser pulse generation. Figure 8(a) presents the PA signal phase delay as function of pressure of pure water vapor in the cell. The value of vibration-translational relaxation time at water vapor pressure of 1 torr was found to be  $\tau_{VT}^0 = (1.78 \pm 0.05) \mu\text{s}\cdot\text{torr}$  from this dependency fitted by formula [16]:  $\phi = \phi_0 + \arctg(\omega \cdot \tau_{VT}^0 / P)$ . Figure 8(b) presents analogous experimental data for mixture of water vapor with air. Note, in region of

pressure more than 15 torr the phase delay increases in direct proportion to pressure because the gas placed in the gap of microphone damps the membrane movement. In analogous PA experiments [17] carried out with the use of amplitude modulated radiation of CW-lasers instrumental phase shift was eliminated by the method of electrostatic activation. Application of such technique in present study is not possible because additional electrode-activator in microphone design [17] will destroyed the pulse PA waveform.

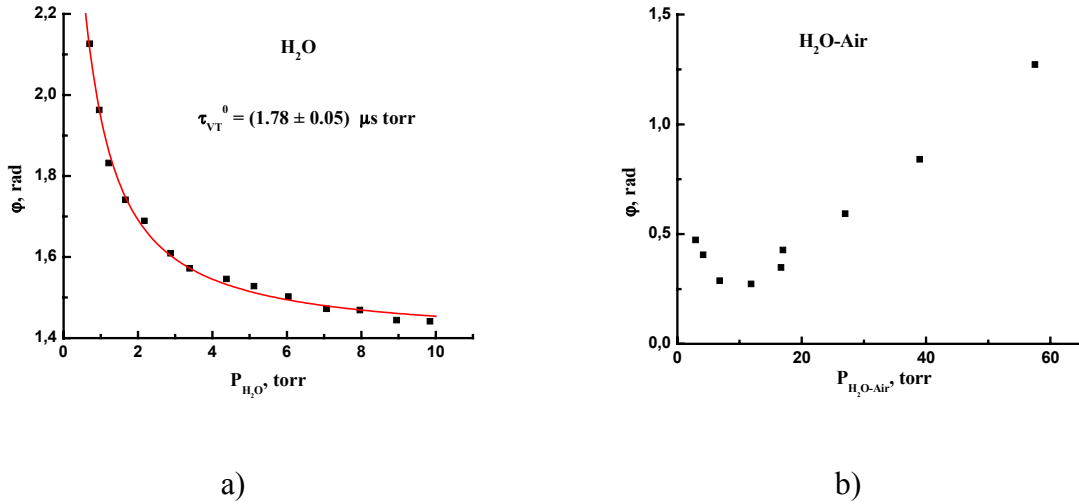


Fig.8. a) - PA signal phase delay  $\phi$  versus the pressure of  $H_2O$  in the cell.  
b) - PA signal phase delay  $\phi$  versus the pressure of  $H_2O$ -Air-mixture in the cell.

Moreover, the correct simulation of pressure pulse influence on membrane by pulse of electrostatic influence on membrane is greatly complicated than simulation in case of slow sinusoidal signal.

### 3.2. Determination of relaxation time for $H_2O$ ( $v_1 + 3v_3$ ) over duration of the pressure signal compression pulse.

It was shown in the papers [6-8] that duration of compression pulse of PA signal depends on the size of laser beam, sound velocity, and heat release time. At low pressure when the laser pulse duration  $\tau \ll \tau_{VT}$  the heat release time is determined by relaxation of excited molecules. So the information about relaxation time can be found, if the shape of pressure pulse  $p(t)$  is restored from the PA electrical signal. Particularly, for Gaussian beam and Gaussian heat release the duration at half-height of compression pulse of pressure signal  $p(t)$  is determined by the simple equation [7]:

$$\tau_{0.5} = 1.316 \sqrt{\tau^2 + \frac{2r_0^2}{V_s^2}}, \quad (5)$$

When all points of the microphone membrane accomplish the same motion, the equation for pendulum forced oscillator may be used to describe the membrane motion at all:

$$\frac{\partial^2 x(t)}{\partial t^2} + 2\beta \frac{\partial x(t)}{\partial t} + \omega^2 x = p(t)S, \quad (6)$$

where  $x(t)$  and  $S$  are the membrane replacement and square;  $\beta$  and  $\omega$  are the damping factor and frequency of membrane oscillation, respectively;  $p(t)$  is the required pressure pulse. After the smoothing of electrical PA signal having the form presented in Fig. 8(a) over the time one order of magnitude smaller than period of oscillations the first and second derivatives were calculated by computer for this signal. The parameters  $\beta$  and  $\omega$  were determined using the unperturbed part of electrical signal (see Fig. 8(b)), as before. After substitution of the oscillation parameters and data on the electrical signal (including the first perturbed part), its first and second derivatives into the equation (6) the signal  $p(t)$  was reconstructed by computer. The shape of signal  $p(t)$  restored for the water vapor pressure of 1.7 torr is presented in Figure 9(a). Figure 9(b) demonstrates how the shape of compression pulse is changed with variation of pressure.

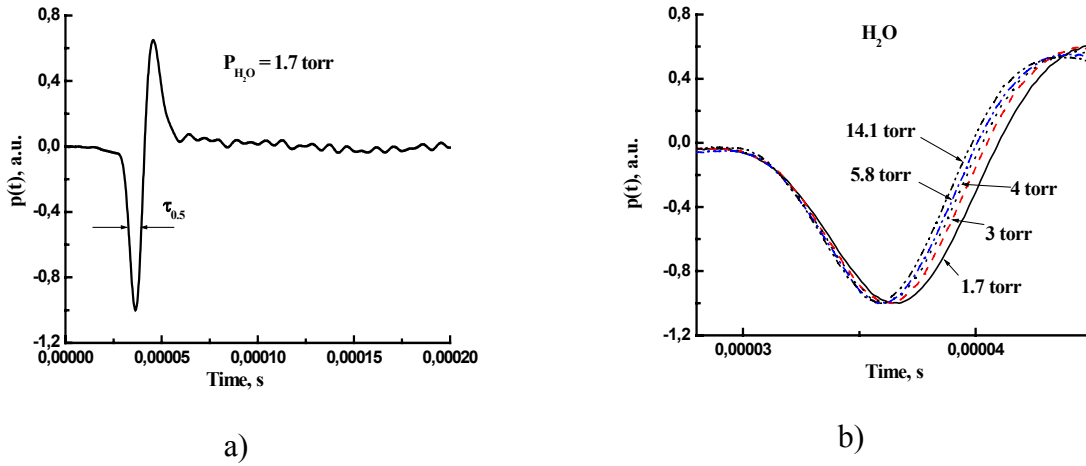


Fig.9. a) - PA signal  $p(t)$  restored from PA detector response.  
b) - The shapes of compression pulses at different values of water vapor pressure.

So, the values of compression pulse duration were determined for each pressure of each gas under study. Figure 10(a) presents the duration of compression pulse versus the pressure of pure water vapor. Dependence  $\tau_{0.5}(P)$  for mixture of water vapor with oxygen is presented in Fig. 10(b). Analogous dependencies were obtained for mixtures of water vapor with nitrogen and air. The values of vibrational-translational relaxation time were found from these dependencies fitted using the formula (5). Good fitting was possible only with allowance for an effect of acoustic-source size increase due to diffusion of exited molecules from radiated area. To do this the effective radius of acoustic source  $r_0'$  was represented as in Ref. [18]:

$$r_0' = r_0 + \frac{5.76 \Delta r_0}{\sqrt{P}}, \quad (7)$$

where  $r_0$  and  $\Delta r_0$  were used as fitting parameters in the equation (5).

To calculate the values of time of water vapor relaxation determined by collisions of  $H_2O$  molecules with molecules of other buffer gases ( $N_2$ ,  $O_2$ , air)  $\tau_{VT}^0(H_2O-M)$ , we used the formula from Ref. [19]:

$$\frac{1}{\tau_{VT}^0(\text{meas.})} = \frac{1}{\tau_{VT}^0(H_2O - H_2O)} X + \frac{1}{\tau_{VT}^0(H_2O - M)} (1 - X), \quad (8)$$

where  $X$  is the water vapor mole fraction in mixture,  $\tau_{VT}^0(\text{meas.})$  is the relaxation time determined for mixture from experimental dependence.

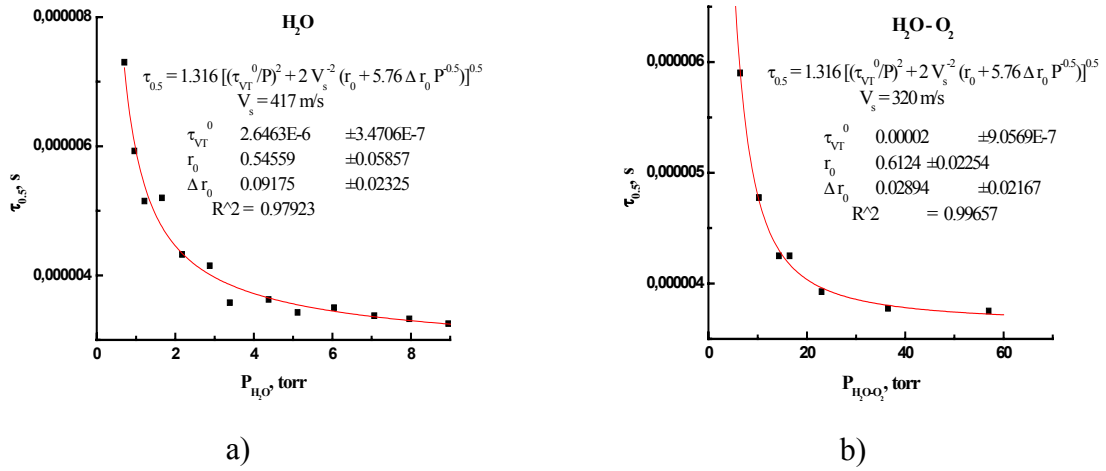


Fig.10. a) - Duration of compression pulse versus water vapor pressure.  
b) - The same for mixture of water vapor with oxygen.

Using the fitting results and equation (8) we have found the next data for relaxation time:

$\tau_{VT}^0(H_2O-H_2O) = 2.6 \mu\text{s}\cdot\text{torr}$ ;  $\tau_{VT}^0(H_2O-O_2) = 29 \mu\text{s}\cdot\text{torr}$ ;  $\tau_{VT}^0(H_2O-N_2) = 14 \mu\text{s}\cdot\text{torr}$ ;  
and  $\tau_{VT}^0(H_2O-Air) = 16 \mu\text{s}\cdot\text{torr}$ .

## ASKNOWLEDGEMENTS

This research was supported in part by Physics Sciences Department of RAS (Basic Spectroscopy Program).

## REFERENCES

1. V.P. Zharov, and V.S. Letokhov, Laser optoacoustic spectroscopy. (Nauka, Moskow, 1984).
2. Photoacoustic, Photothermal and Photochemical Processes in Gases, P. Hess, ed., in *Topics in Current Physics*, (Springer-Verlag, Berlin, 1989).
3. Air Monitoring by Spectroscopic Technique, M.W. Sigrist, ed., (New York, John Willey and Sons Inc., 1994).
4. R.W. Bergstrom, P.B. Russel, and P.Hignett, *J. Atmos. Sci.* **59**:567 (2002).
5. H. Moosmuller, W.P. Arnott, C.F. Rogers, J.C. Chow, C.A. Frazier, L.E Sherman, and D.L. Dietrich, *J. Geophys. Res.* **103(D21)**:28149 (1998).
6. M.S. Dzhidzhoev, V.T. Platonenko, V.K. Popov, and A.V. Chugunov, *Kvantovaya Elektronika (USSR)* **11**:414 (1984).
7. J.-M. Heritier, *Optics Commun.* **44**:267 (1983).
8. I.G. Calasso, W. Craig, and G.I. Diebold, *Phys. Rev. Lett.* **86**:3550 (2001).
9. B.A. Tikhomirov, A.B. Tikhomirov, and K.M. Firsov, *Atmos. and Ocean Optics (Russia)* **14**:740 (2001).
10. I.S. Tyryshkin, Yu.N. Ponomarev, B.S. Mogilnitskii, and B.A. Tikhomirov, *Atmos. Optics (USSR)* **2**:668 (1989).
11. I. Carrer, L. Fiorina, and E. Zanzottera, in *Photoacoustic and Photothermal Phenomena III*, D. Bicanic, ed. (Springer –Verlag, Berlin, 1992) pp. 568-571.
12. B.M. Golubitskii, and M.V. Tantashev, *Izvestiya AN SSSR. Fizika Atmosferi i Okeana (USSR)* **12**:442 (1976).
13. V.S. Kozlov, M.V. Panchenko, A.S. Kozlov, A.N. Ankilov, A.M. Baklanov, and S.B. Malyshkin, in *Proceedings of the Twelfth Atmospheric Radiation Measurement (ARM) Science Team Meeting*, (St. Petersburg, Florida, 2002) p.4.
14. I.S. Tyryshkin, Investigation of line broadening of the atmospheric water vapor in the visible spectral range by high resolution laser spectroscopy, *Ph.D. Dissertation*, (Institute of Atmospheric Optics of USSR Academy of Sci., Tomsk, 1983).
15. A.M. Baklanov, V.S. Kozlov, M.V. Panchenko, A.N. Ankilov, and A.L. Vlasenko, *J. Aerosol Sci.* **29**:919 (1998).
16. V.A. Kapitanov, and B.A Tikhomirov, *Appl. Optics* **34**: 969 (1995).
17. V. Zeninary, B.A. Tikhomirov, Yu.N. Ponomarev, and D. Courtois, *J. Chem. Phys.* **112**:1835 (2000).
18. M. Margottin-Maclou, L. Doyennette, and L. Henry, *Appl. Optics* **10**:1768 (1971).
19. J. Finzi, F.E. Hovis, V.N. Panfilov, P. Hess, C.B. Moore, *J. Chem. Phys.* **67**:4053 (1977).